The Mapping Accuracy Of Low-Cost UAV- Based Laser Scanner System: A Case Study Of Hokuyo Utm30lx Laser Scanner

Anh Thu Thi PHAN, Vietnam
Kazuyoshi TAKAHASHI, Japan

Key words: Laser scanner, UAV, accuracy, low cost, positioning

SUMMARY

A cheap, compact, light- weight UAV- based laser scanner system was developed. The developed system, powered by Pin Lithium Polymer (LiPo), consists of a hex-rotor aircraft DJI S800 with the 3-axis gimbal (TAROT 5D) carrying the Hokuyo UTM30LX laser scanner, an ultra-small motion logger (Ninja Scan Light), GPS receiver and a single-board PC (Raspberry Pi). The test flights in Kumamoto prefecture had been performed in 2014. The point clouds were collected with the setting of a 100^0 of field of view and 0.25^0 of angular resolution at the height of about 7 meters from the ground surface. There were 9 markers arranged within the study area. Their coordinates were measured with total station and used as reference value for accessing the accuracy of generated 3D laser point clouds. The locations of markers were identified, and their observed coordinates were manually measured from the intensity image of observation data. By using magnetic data for determining flight direction and applying Helmert transformation with four ground control points, the developed system could achieve a mapping accuracy of 0.04 m in both horizontal and vertical direction. The results show the capability of generating a large- scale map with the low-cost UAV- based laser scanner system.

The Mapping Accuracy Of Low-Cost UAV- Based Laser Scanner System: A Case Study Of Hokuyo Utm30lx Laser Scanner

Anh Thu Thi PHAN, Vietnam
Kazuyoshi TAKAHASHI, Japan

1. INTRODUCTION

Laser scanning is an effective technology available in many research areas such as photogrammetry, surveyors, architectural restoration. This technique can rapidly capture dense spatial data. In agriculture, ground-based lasers have been popular used for purpose of plant height monitoring (Lumme et al., 2008; Hoffmeister et al.,2010; Zhang and Grift, 2012; Kaizu et al., 2012, Tilly et al., 2012), biomass estimation (Tilly et al., 2013 and 2014; Bendig et al., 2014, Ehlert et al., 2008, 2010 and 2013) or vertical plant area density profile (Hosoi and Omasa, 2009 and 2012). They have demonstrated their useful in precise agriculture, with their ability of collecting a lot of crop information in a short time.

Obtaining the information of the target objects from above can achieve the data in large area, with high resolution and in real time. For this, airborne laser scanners have been developed and applied for terrain mapping and forest inventories (Riano et al., 2003; Lee at al., 2007). The GPS signal receiver provides the aircraft position and an inertial-measurement unit (IMU) device recorded the aircraft altitude. From this, the accuracy of building 3D laser point clouds could be improved. However, this system costs a lot of money for system cost and operation and must be controlled by a trained pilot with takeoff and landing challenges. Additionally, in some country, using of aircraft for surveying or other research purposes encourages strictly regulations from the government.

Nowadays, a growing number of Unmanned Aerial Vehicle (UAV) has been being developed with different weight, payload, endurance and range, speed, wing loading, cost, engine type and power. UAV- based systems have been developed for many purposes with various sensors such as imaging sensor (Sugiura et al., 2005; Hunt et al., 2010; Rango et al., 2009), multispectral sensor (Berni et al., 2009) or LIDAR sensor (Wallace et al., 2012). Such systems inherit the advantage of manned aerial vehicle system. With the developing of light weight laser scanner and positioning instruments (the GPS and IMU sensor), airborne laser scanner can be performed with a UAV. Normal airborne laser scanners weighting a few to several tens of kilograms are installed on large UAV weighting several tens to hundreds of kilograms for mapping purposes (Johnson, 2006; Nagai et al., 2009). Unfortunately, such mentioned UAV and airborne laser scanner, costing several of ten to hundred thousand of dollars, are very expensive. In some situation of studies, lightweight or small-UAVs weighing several kilograms are regulated suitable, less expensive, easier to operate and transportation than heavier UAVs. For these reasons, small UAV-based systems are more flexible and could collect multi-temporal data acquisitions with low costs. For example, several small UAV-based systems weighting approximate and less than 10 kg has been developed for forest inventory (Lin et al., 2011; Zahawi et al. 2015). Because of payload limitation, the compact and light weight sensor are

required for small UAV-based systems. Although flight duration is short, small UAV-based systems have a possibility to observe large target area with multi transects.
In precise agriculture, it is necessary to collect the crop information in individual paddy. The transportation of such heavy and bulky devices to the field is difficult. Small and light weight UAV-based systems demonstrates their useful in such the situations. Such small devices can be manually carried to target fields easily. Thus, a small UAV- based laser scanner system for monitoring agricultural crops is proposed to be developed in this study. This system can fly at low altitude and collect information with high resolution for instant crop condition monitoring. The whole system is easy to be carried because of lightweight and compact devices. Moreover, the developed system incurs the lowest possible cost in order to reduce the initial outlay and running costs of crop-monitoring systems. For developing the system, the horizontal attitude of the laser scanner was maintained by a 3-axis gimbal. The system position was located by a single-frequency GPS receiver. A small device, Ninja Scan Light, was installed to record the magnetic field intensity of the Earth. In this study, both GPS and magnetic data are used to identify the flight direction. The accuracy of building 3D laser point cloud is assessed in specific situations of applying and non-applying correction method with ground control points.

2. SYSTEM DESCRIPTION

To develop the system, the low-cost, compact, and light-weight devices are priority selection (Table 1). In detail, The DJI spreading wings S800 (DJI S800) was selected as platform for the developed UAV-based system (developed system). This is a hex-rotor aircraft specialized for aerial photography. The DJI S800 has 6 brushless motors with carbon fiber propellers. They are respectively assembled in 6 frame arms which are integrated to circuit-integrated center frame. The total platform weighs 2.6 kg and under 7 kg takeoff weight design. The scanner payload was selected based on the total payload limitation design. The chosen line laser scanner, Hokuyo UTM30LX, is designed for robot with higher moving speed because of fast response. This is a compact laser scanner with 0.37 kg of weight, detection range from 0.1 to 30 m with the wide angle of 270^0. The light source emits all wavelengths of 905 nm. For system developing, the scanner was set to have a 100^0 of field of view and 0.25^0 of angular resolution with scan frequency of 40 Hz. The straight and level equilibrium flight is not easy to be achieve with small UAV. During observation flights the UAV altitude is fluctuation, therefore; a 3-axis gimbal (TAROT 5D) was used in order to maintain the horizontal attitude of the line laser scanner. Moreover, a single-frequency GPS receiver (Sensor-Com Kinematic GPS Evaluation Kit) was installed. The post processing kinematic GPS raw data, recorded at a rate of 5Hz, was done in order to locate the airframe position with the highest possible accuracy. Moreover, flight direction information is necessary for computing the coordinate of 3D laser point clouds. Thus, an ultra-small motion logger (Ninja Scan Light) was installed on-board to obtain the magnetic field intensity of the Earth at a rate of 1 Hz. The line laser scanner and the GPS receiver are both controlled by a single-board PC (Raspberry Pi). The observed data was also stored in this Raspberry Pi. Recorded data synchronization was performed using GPS time. Finally, the whole system was supplied the power by Pin Lithium Polymer (LiPo) for capable of flight times of about 5 minutes. The developed system and its devices are clearly illustrated in figure 1.

Table 1: UAV- based laser scanner system components

Components	Prices (USD)	Weight (kg)
DJI S800	3000	2.60
Hokuyo UTM 30LX	3300	0.37
TAROD 5D	1100	0.20
Sensor-COM GPS	50	--
NinjaScan- Light	17	0.02
Raspberry Pi 2	35	0.05
Turnigy 5000mAh 6S 40C (Lipo)	60	0.84
Turnigy 3300mAh 4S 30C (Lipo)	30	0.39

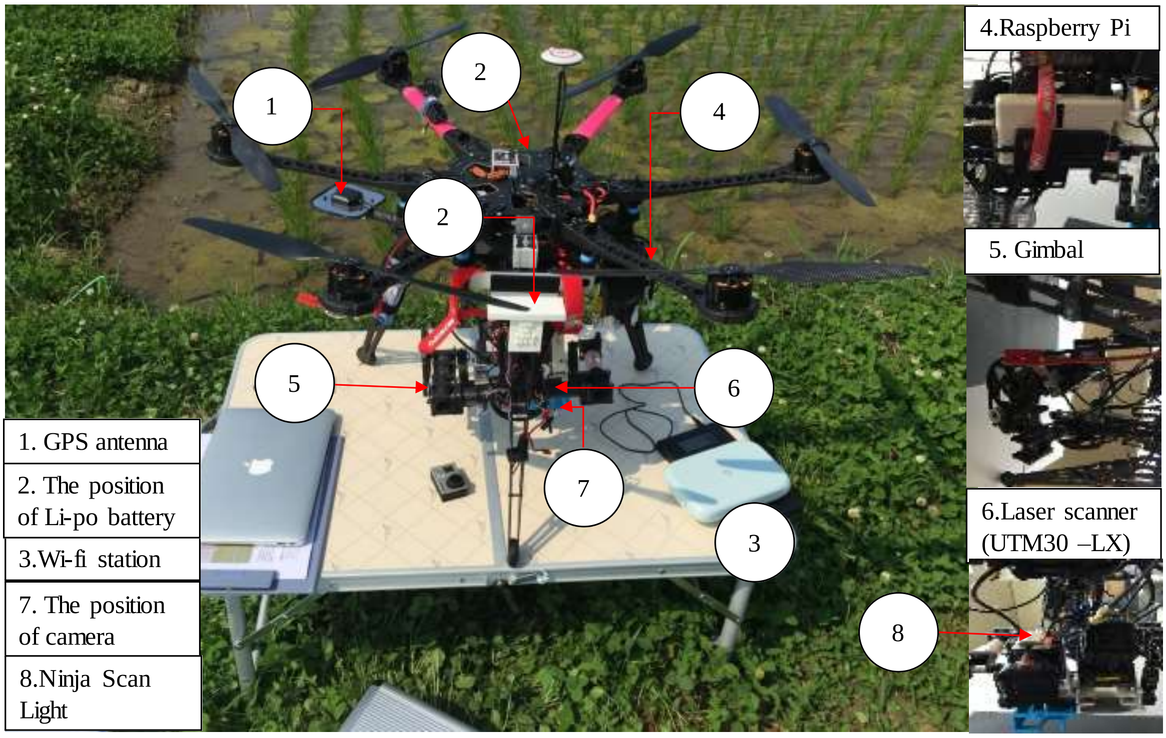

Figure 1: The hex-rotor aircraft DJI S800 with the 3-axis gimbal (TAROT 5D) carrying the Hokuyo UTM30LX laser scanner, an ultra-small motion logger (Ninja Scan Light), GPS receiver and a single-board PC (Raspberry Pi)

3. METHODOLOGY

3.1 3D laser point clouds generation

The laser scanning data captured by the developed system were processed carefully step by step to achieve spatially point clouds. The main purpose of data processing method is to compute the 3D coordinate of laser scanning point cloud in the Japanese mapping coordinate system. For this, the observed data was processed with three main steps: computation of the GPS antenna coordinates in Japanese mapping coordinate system, generation of the 3D coordinates of laser scanning points in laser scanner coordinate system and transformation of laser scanner coordinates to Japanese mapping coordinates.

3.1.1 Computation of the GPS antenna coordinates in Japanese mapping coordinate system (JMCS)

The output of this procedure is the coordinates of GPS antenna in Japanese mapping coordinate system (JMCS). In fact, the Japanese mapping coordinate system (JMCS) consists of 14 individual coordinate systems with different origins. The coordinate system, in this study, is defined with right hand. Based on the location of observation area, the corresponding original point was selected. In this study, the JMCS is modified to right hand coordinate system. In particular, Y-axis of the coordinate system, an axis which coincides with the meridian in the coordinate system origin, urban positive values toward the true north, the X-axis of the coordinate system, an axis orthogonal to the Y-axis of the coordinate system in the coordinate system origin, the true the values toward the West is positive. Scale factor on Y-axis of the coordinate system is 0.9999. To achieve the expected results, the GPS antenna position was firstly located in in global coordinate system. For this, the observed GPS data received by a single-frequency GPS receiver by applying post processed kinematic (PPK) method with RTKLIB version 2.4.1 in order to achieve the GPS antenna geographic coordinates. Then, these coordinates were convert to mapping coordinates in JMCS using Gauss-Krüger projection equations.

3.1.2 Generation of the 3D coordinates of laser scanning points in laser scanner coordinate system (LSCS)

The laser scanner coordinate system (LSCS) was defined as right hand with the origin located at the mechanical origin of the line laser scanner. The Y axis, corresponds to the rotation axis of the scanning mirror and its positive points to moving direction of the scanner. The positive Z points up. The X axis belongs to the scanning plane and its positive points to scanning direction. For illustrating, the 3D coordinates of laser scanning points *t* in LSCS can be express in equation 1 (Figure 2).

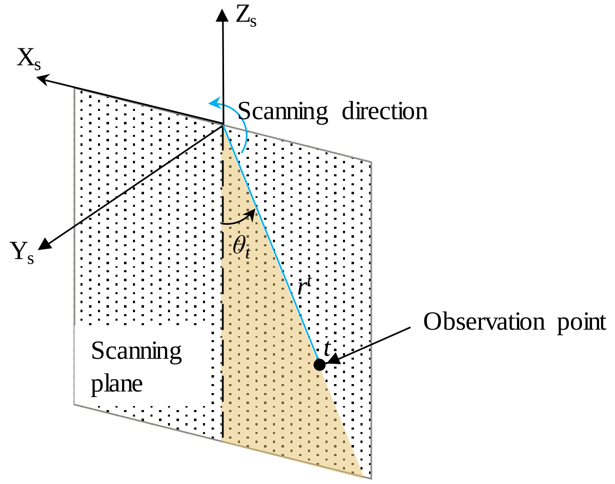

Figure 2: Laser scanning points *t* in laser scanner coordinate system

$$P_t^s = \begin{bmatrix} -r^t.sin\theta_t \\ 0 \\ -r^t.cos\theta_t \end{bmatrix} \qquad (1)$$

Where: P_t^s: The position of target scanning point t in laser scanner coordinate system
r^t: The observed range
θ_t: The scanning angle

3.1.3 Transformation of laser scanner coordinates (LSC) to Japanese mapping coordinates (JMC)

The relative position of LSCS in JMCS is described in figure 3. From this, the coordinates of 3D laser point clouds in LSCS was convert to JMC using the following transformation equation:

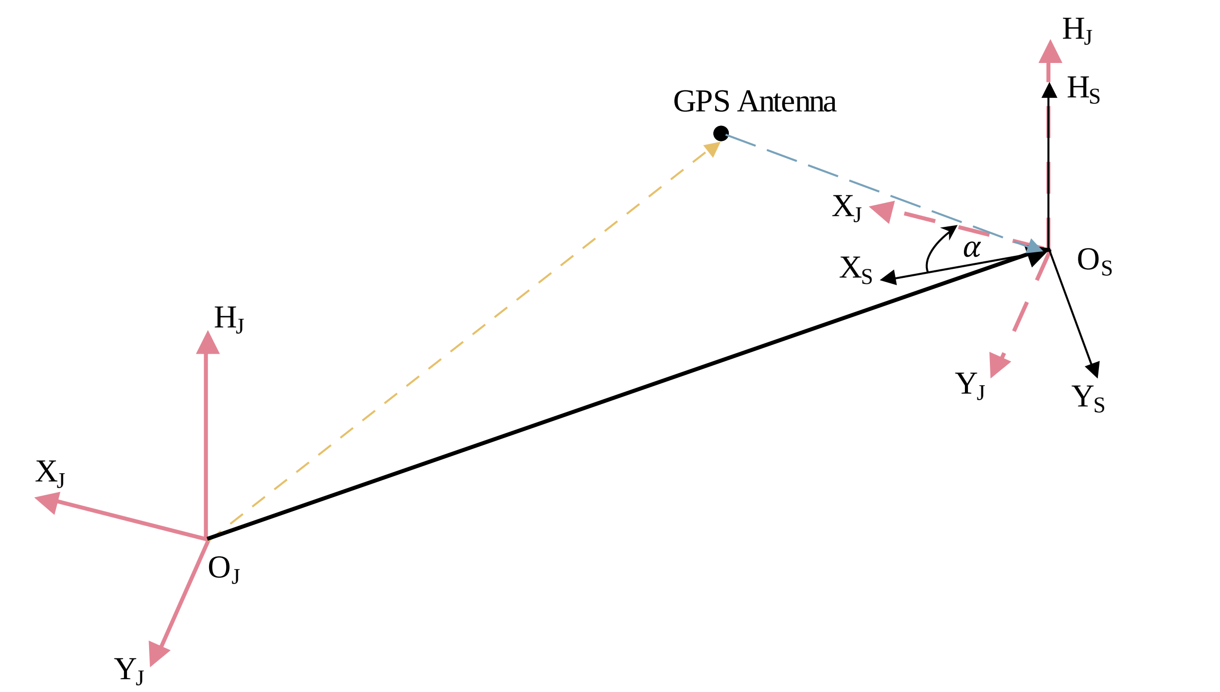

Figure 3: Schematic of transformation of laser scanner coordinate system (O_S X_S Y_S H_S) to Japanese mapping coordinate system (O_J X_J Y_J H_J). α is rotation angle in the horizontal plane

$$P_t^J = (P_{GPS}^J + O_{GPS}^S) + R_s^J P_t^s \qquad (2)$$

Where:
P_t^J: 3D coordinates of laser scanning point in JMCS
P_{GPS}^J: The 3D coordinate of GPS antenna in JMCS
O_{GPS}^S: The offset vector from GPS antenna position to original of LSCS
$(P_{GPS}^J + O_{GPS}^S)$: shows the 3D coordinate of the mechanical origin of the line laser scanner in JMCS
R_s^J: The LSCS to JMCS rotation matrix

P_t^s: The 3D coordinates of laser scanning points in LSCS

Right after getting the GPS antenna coordinates in JMCS, the position of the mechanical origin of the line laser scanner in JMCS is corrected by the value of offset vector (O_{GPS}^S), manual measured with centimeter level of accuracy. Because the horizontal status of the laser scanner is assumed to be maintained by using the gimbal, roll and pitch angles become 0. The rotation matrix (R_s^J), including yaw angle only, is expressed with clockwise rotation angle α. Then, 3D coordinates of laser scanning points are computed by applying the follwing equation

$$P_t^J = (P_{GPS}^J + O_{GPS}^S) + \begin{bmatrix} cos\alpha & -sin\alpha & 0 \\ sin\alpha & cos\alpha & 0 \\ 0 & 0 & 1 \end{bmatrix} P_t^s \qquad (3)$$

3.2 Point clouds accuracy assessment

A flat area located in the campus of National Institute of Technology, Kumamoto College, Kumamoto prefecture in Japan was used as a study area for assessing the accuracy of building 3D laser point clouds using the developed UAV-based system (Figure 4a). The experimental observation performed in Dec. 19th, 2014. As above mentioned, the point clouds were collected with the setting of a 100^0 of field of view and 0.25^0 of angular resolution at the height of about 7 meters from the ground surface. The unstable and gradually increasing of flight altitude caused the significant difference in elevation height of scanning points (Figure 4c).

For accessing accuracy of developed system, 9 markers were arranged within the study area. Their coordinates in JMCS was measured with total station and used as reference value for accessing the accuracy of generated 3D laser point clouds. The locations of markers were identified, and their observed coordinates were manually measured from the intensity image of

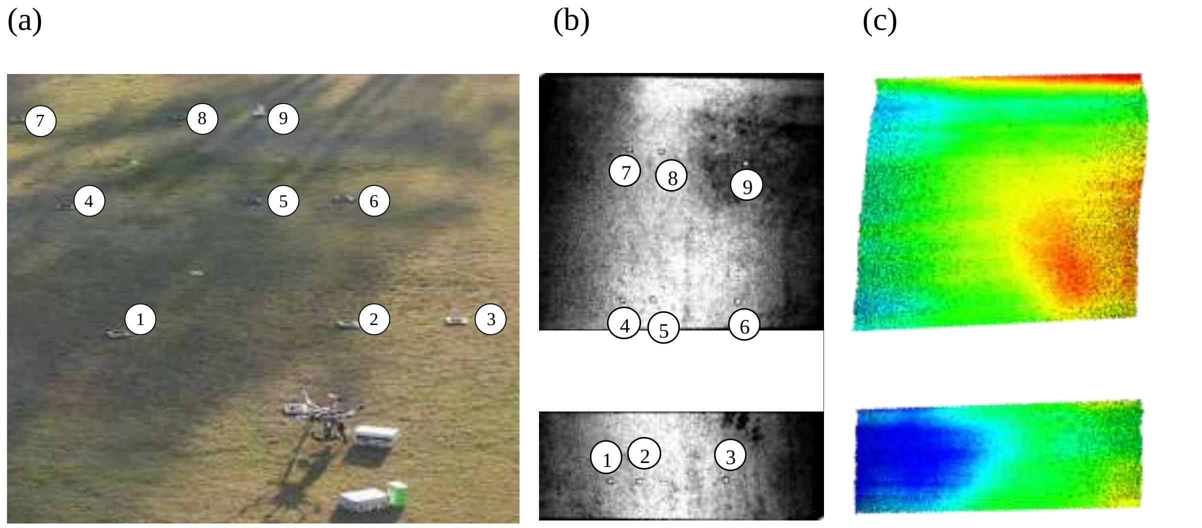

Figure 4: Experimental site. a) The flat study area located in the campus of National Institute of Technology, Kumamoto College, Kumamoto prefecture in Japan. There are 9 markers arranged on the ground surface for validating the accuracy of 3D point cloud generation, b) The intensity images and c) ellipsoid height of scanning points computed from observation data on Dec. 19th,2014 respectively, color coded (red= high, green= low).

observation data. This coordinate was compared with the coordinated measured by the total station to validate the accuracy of developed system. The accuracy was accessed in two individual situations of non-applying translation transformation, and applying Helmert transformation with 4 ground control points.

4. RESULTS

4.1 Trajectory determination

The rotation angle α, in this study, is an important factor for computing the location of laser scanning point (eq. 3). The value of α is identified from the magnetic data recorded by the Ninja scan light. For calibrating the magnetic data, the UAV was turned in circle with the radius of approximated of 1 m. From the magnetic data the magnetic north was identified. From this, the flight direction was identified with the consideration of -6.884 degrees of magnetic declination angle. The rotation angle α, in this study, is determined as the west of north angle between flight direction and the true north direction (Figure 5). In case of uninstalling the Ninja scan light device, the magnetic data could not be recorded. The rotation angle can be computed from the location of UAV recorded by the GPS receiver (Figure 5). According to the result, the rotation angle α ranges from 142.0480^0 to 146.9768^0.

4.2 Point cloud accuracy

The coordinates of scanning points were computed using GPS data. Then, the markers were firstly recognized from intensity images generated from observation data. The marker position was estimated from four scanning points closest to its center. For validating the accuracy of 3D point clouds generation, the observed marker positions were compared to the true position

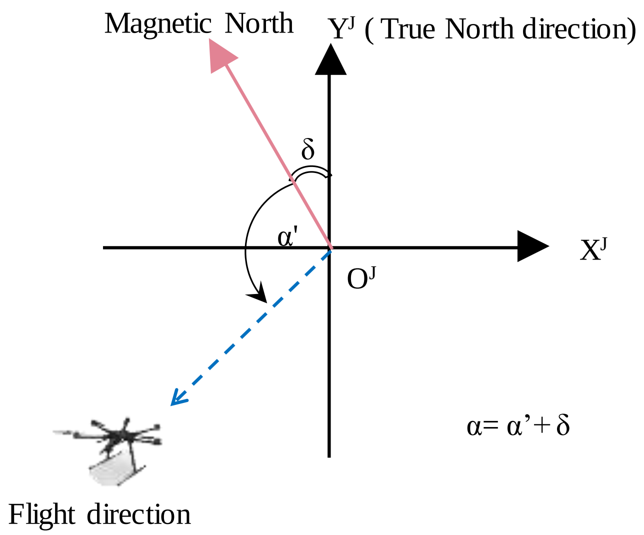

Figure 5: Schematic of identification rotation angle α from magnetic data with α' is the angle computed from calibrated magnetic data and δ is magnetic declination angle

measured by total station. The accuracy of building 3D laser point clouds is assessed by the mean absolute error (MAE) (eq. 4). The MAE values and the standard deviation of the errors are displayed in table 2.

$$MAE = \frac{\sum_{k=1}^{n} |mP_k^L - P_k^L|}{n} \tag{4}$$

Where:

MAE: The mean absolute error
mP_k^L: Measured position of GCP point
P_k^L: Position of the GCP point

Table 2: The accuracy of generating 3D laser point clouds in test flight sites in Kumamoto prefecture, Japan

Orientation data	MAE (m)			Standard deviation (m)		
	Horizontal	Vertical	Spatial	Horizontal	Vertical	Spatial
Magnetic data	1.19	1.09	1.62	0.10	0.09	0.13

With the expectation of improving the horizontal accuracy of building 3D laser point clouds, the Helmert transformation was applied to observation data with four ground control points. With the belief that the farther distance two separated points was selected, the more accurate the result achieved; therefore, four points MP1, MP3, MP7 and MP9 locating at four coners of target field were chosen. As a results of calcualting transformation parameters, the scaling factor is approximate 1.0, and the reotation angles are small. The 3D point cloud is achieved with the mapping accuracy of 0.46 m in horizontal and 0.39 m in vertical. The error of checked points is dispalyed in Table 3

Table 3: The errors of checked points

True coordinate				**Calibrate coordinate**			**Residual**		
ID	**X (m)**	**Y (m)**	**H (m)**	**X (m)**	**Y (m)**	**H (m)**	**X (m)**	**Y(m)**	**H (m)**
MP2	-37001.953	-58136	36.110	-37002.006	-58136.260	36.086	-0.053	-0.016	-0.023
MP4	-36997.702	-58129	36.157	-36997.588	-58128.671	36.204	0.114	0.020	0.047
MP5	-36996.541	-58130	36.135	-36996.422	-58129.491	36.173	0.119	0.037	0.039
MP6	-36993.358	-58132	36.174	-36993.248	-58131.969	36.197	0.110	0.097	0.023
MP8	-36992.083	-58124	36.143	-36992.065	-58123.990	36.132	0.018	-0.037	-0.011

5. Discussion

In this study, using magnetic data for identify the flight direction, the 3D laser point clouds were built with greater precise in the comparison of using the GPS data (Table 4). The horizontal accuracy identified with GPS and magnetic data were 1.19±0.10 m and 1.09± 0.09 m, respectively.

By applying Helmert transformation, in this study, the horizontal accuracy of generating 3D laser point clouds improved. The approximate 1.0 of scale factor and the small rotation angle demonstrate that they need not to be concerned (Table 3). Therefore, translation transformation is suitable for correcting the point cloud generated from the developed system with the spatial accuracy of sub- meter.

In the comparison with previous studies, Sugiura et al. (2005) reported the results of generating map regarding crop status using imaging sensor mounted on the helicopter with spatial error range from 0.18 m to 0.29 m. Johnson (2006) used an UAV-baser laser scanner system for terrain mapping and achieved the results of less than 0.5 m and 1.0 m in vertical and horizontal accuracy, respectively. Wallace et al. (2012) developed a UAV-LIDAR system for forest inventory with horizontal and vertical accuracy of 0.34 m and 0.14 m. In this study, the developed system could achieve a mapping accuracy of 0.46 m in horizontal and 0.39 m in vertical.

Besides the encouraging results, a number of limitations must be improved in future studies. In general, the observation data quality was not good because of many missing scanning lines. Thus, the recording program must be improved to correct this problem. Additionally, the unstable flight altitude caused the less accuracy of generating the point clouds. Moreover, the error in X axis of all check point in the middel target field is more than 1 dm. This result shows that, the UAV was not stable. Therefore, for future study, automatically control mode is suggested to be used instead of manually control mode in order to maintain the flight altitude. Furthermore, the horizontal status of laser was not well maintained. A small test was performed for checking the horizontal status of laser scanner with the continuously test flight including backward movement and without resetting the gimbal. As a result, in such situations, the laser altitude was not stable. To solve this problem, the backward movement should be avoided, and the gimbal is suggested to be reset before performing observational flight. For observing the wide target area with long flight endurance, the horizontal attitude of laser scanner is not easy to maintained in whole flight, the rotation angles adopted by Ninja Scan Light consisting of pitch, roll and yaw angle should be exploited. In this situation, the rotation matrix must be defined with three rotating Eulerian angles.

6. Conclusion

The developed system consists of DJI S800 platform, Hokuyo UTM30LX line laser scanner, a 3-axis gimbal (TAROT 5D), a single-frequency GPS receiver (Sensor-Com Kinematic GPS Evaluation Kit), an ultra-small motion logger (Ninja Scan Light) and a single-board PC (Raspberry Pi). The system weights under 7kg in total and cost approximate 8000 dollars. This is a light-weight and low-cost UAV- based laser scanner system in the comparison with manned aerial vehicle system or heavy UAV- based laser scanner system costing several thousand dollars. The developed system could be manually carried into the target field for investigation and obtain target objects at low altitude.

Although the flight endurance is limited, the developed system shows its capability of multi transects for observing target area. The data can be collected at low altitude with high resolution under cloudy condition. Moreover, such systems are cheaper, more compact, light- weight and flexible to use in the comparison with manned aerial vehicle or heavy UAV-based system. This system is simple installation, easy operation, easily removable and can be manually carried to the target fields. The results confirm that the developed system can be applied for monitoring the rice plant in paddy level.

7. Acknowledgment

This study was partially supported by Ho chi Minh City University of Technology-VNU-HCM under grant number T-KTXD-2018-113.

REFERENCE

1. Berni J. A. J., Zarco-Tejada P. J., Suárez L., and Fereres E. (2009). Thermal and Narrowband Multispectral Remote Sensing for Vegetation Monitoring From an Unmanned Aerial Vehicle. IEEE transactions on geoscience and remote sensing 47 (3), 290-305
2. Bendig J., Bolten A., Bennertz S., Broscheit J., Eichfuss S., and Bareth G.. (2014). Estimating biomass of barley using crop surface models (CSMs) derived from UAV-based RGB imaging. Remote Sensing 6, 10395–10412
3. Ehlert D., Horn H. J., and Adamek R. (2008). Measuring crop biomass density by laser triangulation. Computers and Electronics in Agriculture 61(2), 117–125
4. Ehlert D., Horn H. J., and Adamek R. (2010). Suitability of a laser rangefinder to characterize winter wheat. *Precision Agriculture* **11**, 650-663
5. Ehlert D. and Heisig M. (2013). Sources of angle-dependent errors in terrestrial laser scanner-based crop stand measurement", *Computers and Electronics in Agriculture **93***,10-16
6. Grenzdörffer G.J. (2014). Crop height determination with UAS point clouds. The International Archives of the Photogrammetry, Remote Sensing and Spatial Information Sciences, XL-1, 135-140
7. Hosoi F., and Omasa K. (2009). Estimating vertical plant area density profile and growth parameters of a wheat canopy at different growth stages using three-dimensional portable lidar imaging. ISPRS Journal of Photogrammetry and Remote Sensing, 64, 151–158
8. Hoffmeister D., Bolten A., Curdt C., Waldhoff G., and Bareth G. (2010). High resolution Crop Surface Models (CSM) and Crop Volume Models (CVM) on field level by terrestrial laser scanning. Proc. of SPIE, 6th International Symposium on Digital Earth, 7840
9. Hunt E. R., Hively W. D., Fujikawa S. J., Linden D. S., Daughtry C. S. T. and McCarty G. W. (2010) Acquisition of NIR-Green-Blue Digital Photographs from Unmanned Aircraft for Crop Monitoring", Remote Sensing 2, 290-305
10. Hosoi F., and Omasa K. (2012). Estimation of vertical plant area density profiles in a rice canopy at different growth stages by high-resolution portable scanning LIDAR with a lightweight mirror. ISPRS Journal of Photogrammetry and Remote Sensing, 74, 11–19
11. Johnson P. (2006). Unmanned aerial vehicle as the platform for lightweight laser sensing to produce sub-meter accuracy terrain maps for less than $5/km2. Mech. Eng. Dept., Columbia Univ., New York
12. Kaizu Y., Choi J. M., and Kang T. H. (2012). Grass height and yield estimation using a three-dimensional laser scanner, Environment Control in Biology, 50(1), 41–51
13. Lee A.C. and Lucas R.M. (2007). A LIDAR-derived canopy density model for tree stem and crown mapping in Australian forest. Remote Sensing of Environment 111, 493 – 518
14. Lumme J., Karjalainen M., Kaartinen H., Kukko A., Hyyppä J., Hyyppä H., Jaakkola A., and Kleemola J. (2008). Terrestrial laser scanning of agricultural crops. The International Archives of the Photogrammetry, Remote Sensing and Spatial Information Sciences. XXXVII. B5, 563–566
15. Lin Y., Hyyppä J., and Jaakkola A. (2011). Mini-UAV-Borne LIDAR for Fine-Scale Mapping. Ieee Geoscience And Remote Sensing Letters, 8(3), 426-430
16. Nagai M., Chen T., Shibasaki R., Kumagai H., and Ahmed A. (2009). UAV-Borne 3-D Mapping System by Multisensor Integration. IEEE Trans. Geosci. Remote Sense., 47(3), 701-708

17. Riano D., Meier E., Allgower B., Chuvieco E., and Ustin S. L. (2003). Modeling airborne laser scanning data for the spatial generation of critical forest parameters in fire behavior modeling. Remote Sensing of Environment 86(2), 177–186
18. Rango A., Laliberte A., Herrick J. E., Winters C., Havstad K., Steele C., and Browning D. (2009). Unmanned aerial vehicle-based remote sensing for rangeland assessment, monitoring, and management. Journal of Applied Remote Sensing, 3, 033542
19. Sugiura R., Noguchi N., Ishii K. (2005). Remote-sensing Technology for Vegetation Monitoring using an Unmanned Helicopter. Biosystems Engineering 90 (4), 369–379
20. Tilly N., Hoffmeister D., Liang H., Cao Q., Liu Y., Lenz-Wiedemann V., Miao Y., and Bareth G. (2012). Evaluation of terrestrial laser scanning for rice growth monitoring. International Archives of the Photogrammetry, Remote Sensing and Spatial Information Sciences, XXXIX-B7, 351–356
21. Tilly N., Hoffmeister D., Cao Q., Lenz-Wiedemann V., Miao Y., and Bareth G. (2013). Precise plant height monitoring and biomass estimation with terrestrial laser scanning in paddy rice, ISPRS Annals of the Photogrammetry, Remote Sensing and Spatial Information Sciences, II-5/W2, 295–300
22. Tilly N., Hoffmeister D., Cao Q., Lenz-Wiedemann V., Miao Y., and Bareth G.(2014). Multitemporal crop surface models: accurate plant height measurement and biomass estimation with terrestrial laser scanning in paddy rice. Applied Remote Sensing, 8, 1–22
23. Wallace L., Lucieer A., Watson C. and Turner D. (2012). Development of a UAV-LiDAR System with Application to Forest Inventory. Remote Sensing, 4, 1519-1543
24. Zhang L., and Grift T. E. (2012). A LIDAR-based crop height measurement system for Miscanthus giganteu, Computers and Electronics in Agriculture, 85, 70–76
25. Zahawi R. A., Dandois J.P., Holl K.D., Nadwodny D., Reid J. L., Ellis E. C. (2015). Using lightweight unmanned aerial vehicles to monitor tropical forest recovery, Biological Conservation 186 (2015) 287–295
26. DJI Innovation, Spreading Wings S800 User Manual, http://dl.djicdn.com/downloads/s800/S800_User_Manual_en.pdf accessed on Sep. 6th, 2016
27. Hokuyo Automatic Co. LTD, Communication Protocol Specification For SCIP2.0 Standard http://www.hokuyo-aut.jp/02sensor/07scanner/download/pdf/URG_SCIP20.pdf accessed on Sep. 6th, 2016
28. RTKLIB source program package version 2.4.1 http://www.rtklib.com accessed on Jun.1,2016

CONTACTS

Anh Thu Thi PHAN
Institution: Department of Geomatics Engineering, Faculty of Civil Engineering, Ho Chi Minh University of Technology- Vietnam National University
Address: 268 Ly Thuong Kiet Street , Ward 14, District 10, Ho Chi Minh City, VietNam
Phone number: +84 28-38-655-142
Email: ptathu@hcmut.edu.vn

Kazuyoshi TAKAHASHI
Institution: Nagaoka University of Technology

Address: 1603-1, Kami-Tomioka, Nagaoka, Niigata 940-2188, Japan
Phone number: +81 258 - 47 - 9673
Emails: ktakaha@nagaokaut.ac.jp